Journal of Alloys and Compounds, 195 (1993) 387–394
JALCOM 7491

Critical currents in real HTSC materials

V. M. Pan

Institute of Metal Physics, Kiev 252142, Ukraine

Abstract

It is shown that in $YBa_2Cu_3O_7$ single crystals and highly c-axis oriented thin films the similar screw dislocations induced cooperative mechanism of growth can be observed. Such growth is accompanied by volume rotations of microblocks which result in formation of low-angle subgrain boundaries. Low angle boundaries appeared to be consisting of edge dislocations arrays (walls). Dislocation density of such particular structures actually defines values of critical current density in real HTSC materials.

1. Introduction

Since high temperature superconductors were discovered, an aspiration to use them for high current devices working at high fields and liquid nitrogen temperature stimulated researchers. Nevertheless, despite of intensive efforts, conductors of HTSC materials with high current carrying ability at 77 K are not developed up to date.

Transport J_{c_t} at 77 K and $J_{c_t}(H)$ values, which are necessary for high current application, such as magnet systems, electrical machines, power transmission lines, etc., were reached only in thin epitaxial films. For example, in $YBa_2Cu_3O_{7-x}$ deposited epitaxially onto a single crystalline dielectric substrate the critical current J_{c_t} can exceed $5 \times 10^6\ A/cm^2$ in the self current field [1]. At 5 T field applied perpendicularly to the CuO_2 layers in a c-oriented quasi-single-crystalline YBCO film $J_{c_t}(77K, 5T) \geq 10^4\ A/cm^2$ [2].

In the single crystals grown by the conventional solution-melt procedure [3] the direct critical current measurements are embarrassed because of extremely small sample size (usually $2.0 \times 1.5 \times 0.1\ mm$) and contact resistance. Only very recently we have firmly shown that in the single crystals $J_{c_t}(77\ K)$ can be higher than $10^5\ A/cm^2$ in the self current field [4] and at $2T$ applied perpendicularly to the c-axis $J_{c_t}(77\ K, 2\ T) \geq 2 \times 10^4 A/cm^2$ [4].

As for the bulk conductors, that is wires (single and multifilament) as well as tapes, $J_{c_t}(77\ K)$ in such materials does not exceed $1 \div 5 \times 10^4\ A/cm^2$ and at 5 T field applied parallel to the c-axis hardly reach $10^3\ A/cm^2$.

Thus, difficulties with applications of high current HTSC materials at 77 K have been found to be rather significant. Likely, much more efforts are required to overcome these obstacles.

The problems have been found to be connected with a layered crystal structure, which determines anisotropic properties of HTSC compounds. It is well known that HTSC materials can be described as a pile of superconducting CuO_2 layers separated from each other with layers of different atoms constituting an insulator. The supercurrent flow in such anisotropic structure is confined within CuO_2 (ab) planes.

The anisotropic layered structure of HTSC materials and their extremely short coherence length lead to a serious problem on the way to achieve high $J_c(77\ K)$ and $J_c(H)$. Indeed two basic contradictory conditions are to be satisfied: (i) Material structure must consist of continuous CuO_2 planes highly oriented along the direction of the transport supercurrent. (ii) High density of structure defects must be introduced into material to provide the strongest pinning of Abrikosov vortices, but without any distortions of stacking of CuO_2 planes, coupling, and continuity.

The most effective pins appear to be extended linear defects (dislocations) along applied magnetic field. Twenty years all researchers considered single dislocation as a defect which cannot provide strong pinning. However, the case of HTSC is quite different because the dislocation core size and the coherence length in ab-plane have the same length scale. The core interac-

0925-8388/93/$06.00

© 1993 – Elsevier Sequoia. All rights reserved

tion mechanism leads to extremely strong vortex pinning which could be enhanced by electrostatic interaction [5].

Observed distinction of the transport critical current density in YBCO single crystals and YBCO laser ablated or magnetron sputtered quasi-single-crystalline thin films can be explained by a considerable difference of edge dislocation density at subgrain boundaries.

The similar cooperative growth mechanism mediated by screw dislocations and formation of polygonized spirals and volume rotations seem to be responsible for the formation of a large number of slightly misoriented subgrains both in YBCO single crystals and thin films. However, the dislocation density in thin films has been shown to be much higher $\geq 10^{11}\ cm^{-2}$ against $\sim 5 \times 10^9\ cm^{-2}$ in single crystals.

2. Single crystals

YBCO single crystal were obtained by conventional flux melt growth technique in YSZ crucibles. In contrary to the results of all previous measurements of the transport critical current density in our studies [4] J_c and $J_c(H)$ were at least by an order of magnitude higher than J_{ct} which was measured earlier by other authors.

The results of J_c measurements for different crystals are listed below.

Table 1. Critical currents of the single crystals

Crystal number	T_c, K $(R = 0)$	J_c, A/cm^2	T_{meas}, K
6A	87.0	7×10^4	81.2
7A	88.3	2×10^5	82.5
10A	86.0	4×10^4	83.2
1B	87.5	1×10^5	82.0

Data measured by us for crystals are presented in Fig.1(a,b): temperature and field dependencies of J_{ct}. Resistivity at 100 K approximately 50 $\mu\Omega \cdot cm$, resistivity ratio $\rho_{300}/\rho_{100} \geq 3$, the average mosaicity in ab-plane (measured by X-ray) less than one angle degree, mosaic block size of $0.7 \div 0.8\ \mu m$ as estimated from X-ray data. Transport electrical measurements were carried out on chemically etched very thin bridges with cross section area about $400 \div 500\ \mu m^2$ with the use of permanent and pulse current ($2\ \mu s$ pulse duration, repetition frequency 50 Hz). More details of the J_c measurements were described elsewhere [4].

It was quite natural to suggest that such high measured J_{c_t} and $J_{c_t}(H)$ are due to some features

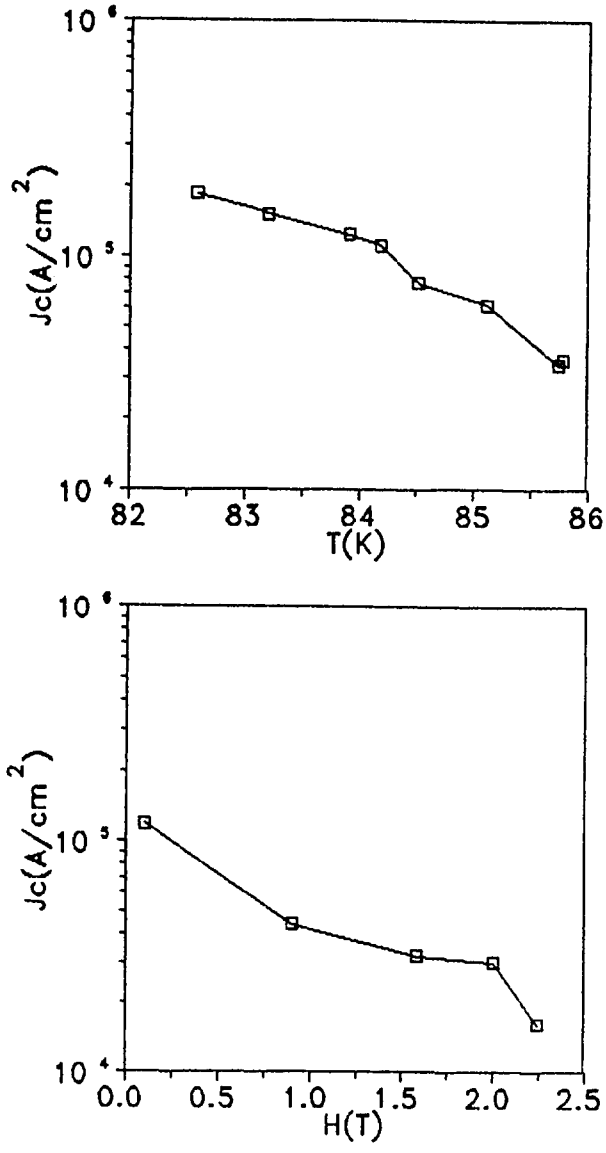

Figure 1(a,b).

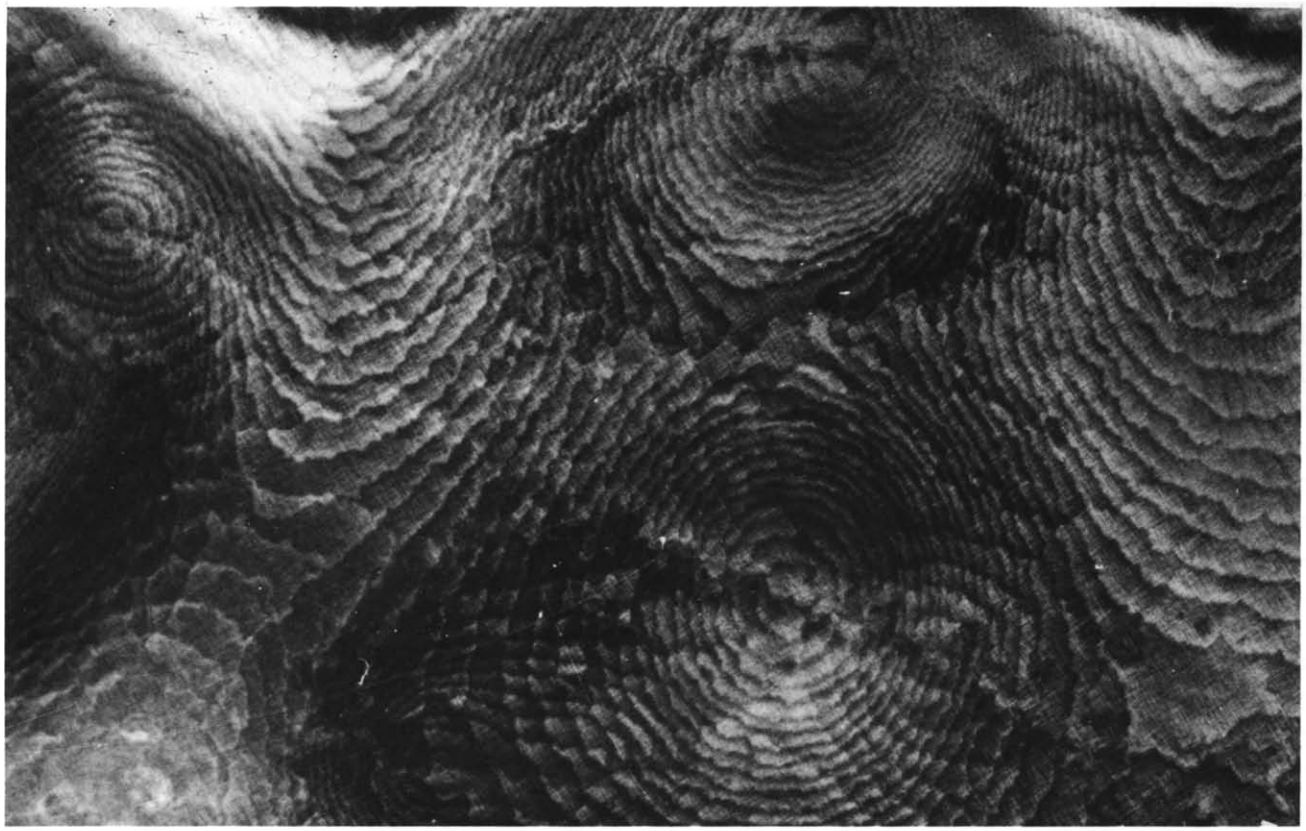

Figure 2. Growth spirals and microblocks in YBCO crystal.

of the fine structure of these crystals. We used TEM and HREM to study microstructure [6].

Samples for TEM and HREM studies were two-side ion-milled with rotation under the argon ion beam angle of 25° and accelerating voltage of 3.5 kV.

A chemical etching revealed hills or hillocks on the surface of grown crystals. The nature of such phenomenon is purely dislocational (or stress-strain dependent) that has been shown by Hirosawa [7]. Our investigations have shown that ion-milling under high angles acts like chemical etching on YBCO single crystals revealing the same hillocks as the scanning tunneling microscopy does. The structure of the crystals has been examined by TEM and HREM at different magnifications (up to direct resolution of the crystal lattice).

Under the low magnification the HREM image of the etched crystal exhibited contrast like several concentric circles originated from different sources. The HREM micrograph (Fig.2) was observed in a narrow range of a goniometer stage angles exhibiting contrast which is rather crystallographic than topographic one. The shape of the mentioned srtuctural features still reminds hillocks ("pyramids") consisted of several terraces. There were no possibility to detect a sign of "pyramids" respectively (001) plane by electron microscopy. Obviously there were parallel tracks of the mirror plane through the all the apexes of "pyramids". By microdiffraction these tracks were found to be parallel to [100] or [010] directions (no distinction between a and b directions was made in this work). The specific structural features described above had the local density of 10^7 cm^{-2} were nonuniformly distributed in the crystal. In general the picture (Fig.2) is very similar to a interference pattern of several wavy sources. This interference pattern seems to be

"frozen" in YBCO crystal structure. The interaction between circular waves determines the shape of terraces and blocks.

As the magnification increases, the size of microblocks can be measured. The average block size was $0.1 \div 1\ \mu m$. The "tweed-like" structure along [110] direction is observed inside the blocks. This structure is typical for a rearrangement of stresses in YBCO as described in [8,9]. The boundaries between the blocks are low-angle ones. Indeed, "tweed-like" components of the structure change their orientation across the grain boundary about one degree. The latter is confirmed by microdiffraction where all reflections have small in-plane (001) misorientation. It is known that for (110) twinning the azimuthal misorientation is observed for certain crystallographic reflections [8]. This does not occur in our case. Hence, showing the subgrain misorientations, the microdiffraction corresponds to a "domain-like" structure rather than to the "twin-like" one.

The investigation of crystal defects were performed under the highest magnification ($\sim 10^6$). A majority of (001) plane views showed regular crystal lattice without $a/2$ ($b/2$) shifts.

Taking into account the traces of the mirror planes on the spiral apexes (parallel to [100] direction) one can suggest that in YBCO single crystals the spiral growth is accompanied by antiphase boundaries formation. The vertical component of the antiphase boundaries shift vector is responsible for the vertical step formation between terraces of the growth spirals.

Thus, one can conclude that growth spirals as well as microblocks do form the structure of YBCO single crystals. The presence of low-angle microblock boundaries means that there are a [100] (or b [010]) edge dislocations. Therefore, the expected edge dislocations density should be about $10^9\ cm^{-2}$. The contribution to the dislocation density is suggested to be caused by screw dislocations inside the spirals, by edge dislocations at the low-angle microblocks, and by the partials due to the formation of antiphase boundaries. This ensures strong pinning of vortices and results in the highest J_c values known for YBCO single crystals.

3.Thin films

The YBCO films were deposited with the use of a pulsed $Nd:YAG$ laser (wavelength $1.06\ \mu m$) on YSZ (Y-stabilized zirconia) substrates heated to $680 \div 800°C$.

The film thickness were $200 \div 400\ nm$, $T_c \approx 89 \div 93\ K$, the residual resistance $\rho_{100} \approx 100 \div 200\ \mu\Omega \cdot cm$ and the resistance ratio $\rho_{300}/\rho_{100} \approx 2.6 \div 3.0$.

The structure was investigated by XRD, SEM, TEM and HREM methods. Electrical transport measurements of films ($\rho\ (T)$, $\rho\ (T,H)$, $I-V$ characteristics included those in magnetic field normal to the substrate and film) were carried out with the use of a pulsed method. Special features of these measurements and results have been earlier described [10]. The highest critical current density ($J_c(77\ K) \geq 5 \times 10^6\ A/cm^2$) was detected in the film deposited at $T_s = 740°C$.

In the early stages of film nucleation and growth when T_c is high enough ($T_c \geq 740$°C, c-axis oriented islands are formed [11,12] which interconnect at thicknesses of about 5 nm with the proceeding of the deposition process [11]. The island growth follows mechanisms associated with spiral morphology formation. The growth of spiral-like pyramidal islands induced by screw dislocations was first observed in [13,14] with the use of scanning tunneling microscopy (STM). We have managed to detect spiral-like pyramids with the use of conventional scanning electron microscopy (SEM). Such formations described in detail in [15]. As a rule, the islands with pyramidal terraces we detected in this work significantly differ from those observed in [11,13,14] with the use of STM. The visible steps comprise about 10 c-axis unit cells, each $\sim$ 1.2 nm high. In [15] a suggestion is made on the nature of such morphology. The laser ablated films we investigated were obtained with the use of $Nd:YAG$ laser with a wavelength much longer (by a factor of $3 \div 4$) than that generated by an excimer laser, *e.g.* KrF laser ($\lambda = 248\ nm$). This may account for the increased density of screw dislocations in the growing film which may alter in accordance with the spiral growth mechanism [16,17]. In the case where the distance between the dislocation

sources becomes shorter than critical [18]

$$r \ll r_{critical} = \frac{k'\alpha\gamma}{kT\delta}$$

(where γ is the boundary free energy, α is the lattice constant, δ is the supersaturation degree, $k' = 9 \div 6$ for different spiral shapes), the growth induced by individual screw dislocations is replaced with the cooperative growth associated with several dislocation sources simultaneously. According to [16] this growth mode was named "polygonized spiral growth".

Thus, the concentration of screw dislocations in [19] appears to have been evaluated inaccurately. Since it can be assumed that in that case the mechanism of growth of YBCO films was also associated with propagation of polygonized spirals, the actual concentration of screw dislocations was several times higher.

An important feature of this growth mechanism is the initiation of the so called "volume rotations" on a relatively large scale inside the crystal. The shape of the rotating volume "wind" approximates to an Archimedian spiral but depends on the rate of spiral propagation [16]. The volume rotations shown *e.g.* in Fig.3 (TEM photograph) bring about the development of a substructure involving the formation of blocks (subgrains) and low-angle dislocation boundaries, which appear to be dominating structural elements determining the behavior of transport superconducting properties.

It is worth noting that during the growth and structural formation of *c*-axis oriented films in addition to low-angle dislocation boundaries, high-angle boundaries may also arise which, can be described by rotations around the *c*-axis [001] and represented in terms of near-coincidence site lattices (CSL) for orthorhombic crystals. It is assumed that the forming high-angle [001] tilt boundaries represented in the CSL or near-CSL by the values $\Sigma = 1, 5, 13, 17, 29$ may be classified based on energy considerations as special boundaries.

We have shown [15] that in the film deposited at $T = 760°C$ a special boundary with a misori- near-CSL is formed which was determined from the SAD data.

Several authors (see *e.g.* [20]) suggest that high-angle special boundaries may prove more transparent for strongly coupled non-Josephson supercurrents due to their low boundary energy and coherence. Experimental evidence in favour of such a suggestion is assumed to have been obtained in work [21] carried out on $YBa_2Cu_3O_{7-x}$ bicrystals misoriented at various angles relative to each other. However, for the present these data cannot be considered unambiguous. The complete transparence for strongly coupled supercurrents has been convincingly demonstrated in one high-angle boundary only: the 90° [010] twist boundary [22].

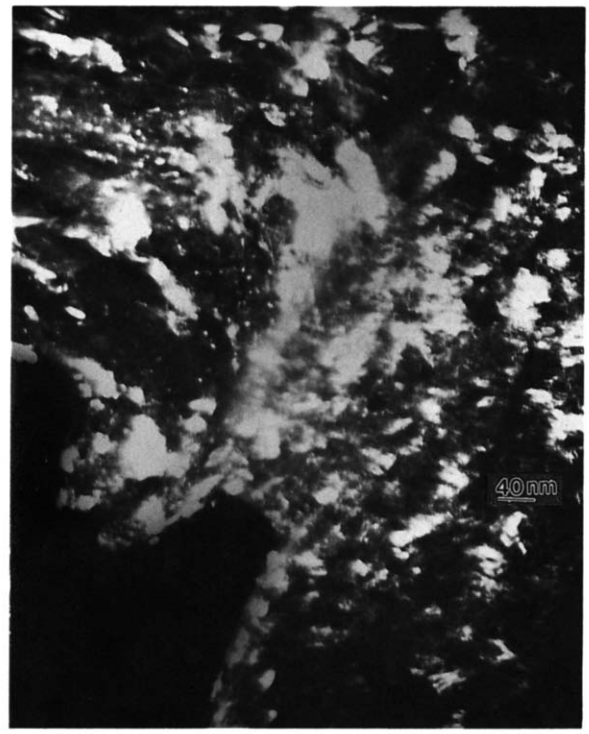

Figure 3. Macro-spiral close to the interface with YSZ substrate formed in the film deposited at $T_s = 740°C$ (dark-field image). Each "wind" corresponds to a separate screw dislocation.

It is worth noting that in several films deposited on YSZ substrates at $T > 760°C$ no high-angle boundaries were observed by SAD and X-

ray analysis methods.

Similar results were obtained in other works (see *e.g.* [23]). The reasons for inducing the formation of the quasi-single-crystalline structure in films where only low-angle dislocation boundaries of the subgrains are present remain unclear. However, an important role in the formation of such quasi-single-crystalline structures has been ascribed to the artificial epitaxy or graphoepitaxy phenomenon [12,23,24].

A question arises on the effective pinning centers in films with a quasi-single-crystalline structure. The authors of [13,14] were the first to suggest that high density growth screw dislocations ($n_d \approx 10^9\ cm^{-2}$) serve as effective pinning centers. However, the density $n_d \approx 10^9\ cm^{-2}$ is not sufficient to account for high $J_c(H)$ in fields with induction of 1 T, when the average vortex density $B/\phi_0 \approx 5 \times 10^{10}\ cm^{-2}$. The most significant role in the density of pinning centers may be played by edge dislocations with the Burgers vector $b = a$ [100] which form the grain or subgrain boundaries and the concentration of which (depinning on average grain size and misorientation) can reach or even exceed [12,19] $10^{11}\ cm^{-2}$.

The structure of the low-angle tilt 3.5° boundary has been recently studied by high resolution electron microscopy [25]. The authors have shown that it consists, as was mentioned above, of a number of discrete edge dislocations. The spacings of these dislocations, D, gives $\sim 6\ nm$ and corresponds to the known Frank formula, $D = |b|/\sin\theta$ or $D = |b|/\theta$ for low θ.

The dislocation cores are of a finite size, about 2 nm in diameter. It should be noted that areas in low-angle boundaries separated from each other by highly located cores reveal a perfect lattice connectivity and a considerable number of practically undistorted rows of $Cu - O$ atoms which appear to be able to provide the flow of strongly-coupled (non-Josephson) supercurrent through the boundary. The flow of strongly coupled current through the boundary is cut off when the dislocation cores form a continuous row, *i.e.* the distance D is equal to $\sim 2\ nm$. It is easy to see that this distance exactly corresponds to the critical misorientation angle value of 10° found in [26].

These assumptions make it possible to explain the origin of the Josephson characteristics of the grain boundary and the magnitude of the critical misorientation angle at which the transition from strongly coupled to Josephson behavior of the grain boundary occurs.

The fast decrease in the critical current values with an increase in grain misorientation angle within the interval below $10° \div 11°$ observed in [26] on bicrystalline films may be associated in our opinion with local suppression of the superconducting order parameter along the dislocation chain forming the boundary, due to the proximity effect which, as we suppose, arises on the boundary between superconducting and non-superconducting areas in the vicinity of the dislocation core. With an increase in the grain misorientation angle and closing in of edge dislocation cores along the boundary, so called easy slip channels for vortex motion are formed which appear during the investigation of the films' $I-V$ curves, as we have shown *e.g.* in [19].

4. Linear defects and vortex pinning

As was mentioned before, at relatively low misorientation angles the edge dislocations along the grain boundaries and other linear defects may act as effective pins and determine high values of critical current density. It should be noted that in the experiment it is rather difficult to determine unambiguously the type of main pinning centers. Nevertheless, based on the analysis of field functions of pinning forces it has been shown [27] that the main pins in $Y_2Ba_4Cu_8O_{16+x}$ films investigated in that work were dislocations and not *e.g.* point defects. Investigation of the magnetic properties of $YBa_2Cu_3O_7$ single crystals irradiated with heavy ions [28] has revealed that the critical current is determined by vortex pinning on radiation tracks: linear defects arising during irradiation and replacing in this case the dislocations.

These experiments of Civale *et al.* [28] have shown that in $YBa_2Cu_3O_7$ single crystals after

irradiation by heavy ions the ions create channels of damaged material (with diameter $d = 50$ Å) along their tracks. In experiments [28] these channels were aligned parallel the the c-axis of crystal and to magnetic field field $\vec{B}$ and so they could serve as almost ideal pins. It seems to be quite obvious that linear defects of other type (such as screw or edge dislocations) may also serve as effective pins, provided they have a normal core with radius $r \geq \xi_{ab}$.

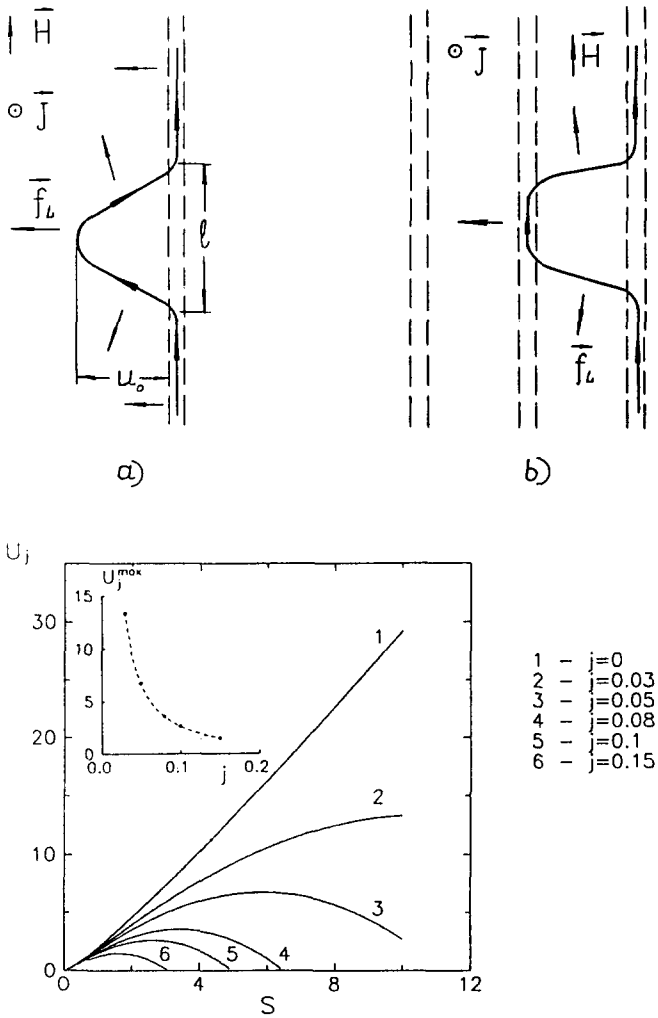

Figure 4. (a) Excited state of the vortes pinned on a linear defect as a "bubble"; (b) vortex transtion from one linear defect to another due to movement of kinks; (c) plot of $U_j(S)$ for different values of reduced current $j = J/J_{co}$. In the insert the maximum value of $U_j(S)$ designated as U_j^{max} is plotted against j. $S = l/\xi_{ab}$.

Basing on the theory of elastic properties of the flux line lattice in anisotropic superconductors [29] in the low field limit, we have calculated the excitation energy of a vortex pinned by a linear defect in anisotropic superconductor carrying transport current J. For an excitation, which has the shape of a linear "bubble" flowed out from the linear defect, its energy [30]:

$$U_j \approx \varepsilon_0[l + a_1 u_0^2/l + a_2(u_0^2 \ln l)/l - a_3 J/J_{c0}(u_0 l)]$$

where l and u are characteristic dimensions of the "bubble" along and across the linear defect respectively. ε_0 is the linear density of the pinning energy:

$$\varepsilon_0(H_c^2/8\pi)\pi\xi_{ab}^2 = \phi_0^2/(64\pi^2\lambda_{ab}^2)$$

J_{c0} is the critical current density in the absence of flux creep:

$$J_{c0} = c\varepsilon_0/(\phi_0\xi_{ab}) = c\phi_0/(64\lambda_{ab}^2\xi_{ab})$$

$a_{1,2,3}$ are numerical coefficients depending on the anisotropy parameter $\gamma = (m_c/m_{ab})^{1/2}$. Analysis of the expression for U_j allows to conclude that in the presence of transport current J there is a critical size $u_0^{max}(J)$ for the "bubble" of optimal shape (corresponding to a minimum of U_j when one of the linear dimensions, *e.g.* u_0, is fixed). If $u_0 \geq u_0^{max}(J)$, the "bubble" becomes unstable. Under the action of the Lorentz force it starts swelling until it will reach the adjacent linear defect. Then, the remaining part of the vortex escapes from the linear defect, where it was pinned, due to the movement of kinks running in the opposite direction along the axis of linear defect. One can also conclude that the activation energy for such kind of vortex depinning should considerably depend on the transport current density even in the low current region $j = J/J_{c0} \to 0$: $U(j) \propto j^{-1}$. This can be observed experimentally as a non-linearity of $I-V$ curves: $E \propto \exp -\alpha/j$. Such kind of non-linearity is often observed experimentally and it is usually ascribed to an influence of collective effects on the vortex lattice (vortex glass state). In the framework of this model such kind of $I-V$ curves may be obtained without taking into account collective effects and it is purely

due to the specific mechanism of the vortex depinning from linear defects. Recently similar results were also obtained by Brandt [31] and Nelson [32].

5. Conclusion

Real structure and substructure of YBCO single crystals and thin films appeared to be much more sophisticated than one could suggest before. Slightly misoriented microblocks in *ab* plane inherited after cooperative spiral mechanism of growth and their dislocation low-angle boundaries give a dominant contribution to flux pinning and critical current density in real YBCO materials.

References

1 V. M. Pan, V. G. Prokhorov, G. G. Kaminsky *et al.*, High-Temperature Superconductors: Material Aspects, DGMI Verlag, FRG, Vol. 1 (1991) 51.

2 V. M. Pan, S. V. Gaponov, G. G. Kaminsky *et al.*, Cryogenics, 29 (1989) S392.

3 V. S. Mel'nikov, V. M. Pan, V. F. Solovjov, and V. F. Taborov, Proc. 3rd German-Soviet Bilateral Seminar on High-Temperature Superconductivity, Karlsruhe, October 8-12 (1990) 664.

4 V. M. Pan, V. F. Solovjov, and V. F. Taborov, Supercond. Sci. Technol., 5 (1992) S192.

5 V. M. Pan, E. A. Pashitski, and C. G. Tretiatchenko, Supercond. Sci. Technol., 3 (1990) 572.

6 V. M. Pan, V. L. Svetchnikov, V. F. Solovjov *et al.*, to be published in Supercond. Sci. Technol.

7 T. Hirosawa, K. Honda, and T. Shibuya, J. Cryst. Growth, 24/25 (1974) 484.

8 Y. Zhu, M. Suenaga, and A. R. Moodenbaugh, Phyl. Mag. Lett., 62 (1990) 51.

9 T. Krekels, G. van Tendeloo, D. Broddin *et al.*, Physica C 173 (1991) 361.

10 V. M. Pan, A. L. Kasatkin, M. A. Kuznetsov *et al.*, AIP Conf. Proc. 251, Buffalo, NY (1991) 603.

11 H. V. Krebs, Ch. Krauns, X. Yang, and U. Geyer, Appl. Phys. Lett., 59 (1991) 2180.

12 S. K. Streiffer, B. M. Lairson, C. B. Eom *et al.*, Phys. Rev. B, 43 (1991) 13007.

13 C. Gerber, J. G. Bednorz, J. Mannhart, and D. G. Schlom, Nature, 350 (1991) 279.

14 M. Hawley, I. D. Raistrick, J. G. Beery, and R. J. Houlton, Science, 251 (1991) 1587.

15 V. L. Svechnikov, V. M. Pan, and H. W. Zandbergen, to be published in Supercond. Sci. Technol.

16 E. Budevski, G. Staikov, and V. Bostanov, J. Cryst. Growth, 24 (1975) 316.

17 C. Nanev, J. Cryst. Growth, 35 (1976) 113.

18 B. N. Sun, K. N. R. Taylor, B. Hunter *et al.*, J. Cryst. Growth, 108 (1991) 473.

19 V. M. Pan, G. G. Kaminsky, and A. L. Kasatkin, Supercond. Sci. Technol., 5 (1992) S48.

20 S. E. Babcock, X. Y. Cai, D. L. Kaiser, and D. C. Larbalestier, Nature, 347 (1990) 167.

21 S. E. Babcock, N. Zhang, Y. Gao *et al.*, J. Adv. Sci., 4 (1992) 119.

22 C. B. Eom, A. F. Marshall, Y. Suzuki *et al.*, Nature 353 (1991) 544.

23 B. H. Moeckly, D. K. Lathrop, S. E. Russek *et al.*, IEEE Trans. Magn., 27 (1991) 2.

24 V. M. Pan, Studies of High Temperature Superconductors, Vol. 5, A. Narlikar (eds.), Nova Sci. Publ., New York (1990) 319.

25 Y. Gao, K. L. Merkle G. Bai *et al.*, Ultramicroscopy, 37 (1991) 326.

26 D. Dimos, P. Chaudhari, and J. Mannhart, Phys. Rev. B, 41 (1990) 4038.

27 P. Berghuis, P. H. Kes, B. Dam *et al.*, Physica C, 167 (1990) 348.

28 L. Civale, A. D. Harwick, T. K. Worthington *et al.*, Phys. Rev. Lett., 67 (1991) 648.

29 A. Sudbø and E. H. Brandt, Phys. Rev. Lett., 66 (1991) 1781.

30 V. M. Pan, A. L. Kasatkin, V. L. Svechnikov, and H. W. Zandbergen, Proc. Int. Conf. "Critical Currents - 92", Vienna, 1992 (to be published in Cryogenics)

31 E. H. Brandt, Europhys. Lett., 18 (1992) 635.

32 D. R. Nelson and V. M. Vinokur, Phys. Rev. Lett., 68 (1992) 2398.